Maleic Anhydride Grafted Thermoplastic Elastomer as an Interfacial Modifier for Polypropylene/Polyamide 6 Blends

Yuchun Ou,[1] Yuguo Lei,[2] Xiaoping Fang,[1] Guisheng Yang[1]

[1]*State Key Laboratory of Engineering Plastics, Center for Molecular Science, Institute of Chemistry, Chinese Academy of Sciences, Beijing 100080, China*
[2]*Shanghai Genius Advanced Materials Company, Limited, Shanghai, 201109, China*

Received 30 December 2002; accepted 11 June 2003

ABSTRACT: A maleic anhydride grafted thermoplastic elastomer (TPE_g) was prepared. The effect of the TPE_g on the morphology and performance of polypropylene (PP)/polyamide 6 (PA-6) blends was studied. The final properties of the blends were tuned through variations in the TPE_g/PA-6 ratios and TPE_g and PA-6 percentages in the blends. Scanning electron micrographs showed that the TPE_g greatly improved the homogeneity of the blends, and this led to better mechanical performance. The nonisothermal crystallization behaviors of PP and PA-6 in the blends, revealed by differential scanning calorimetry, were different from those of pure PP and PA-6. The crystallization temperature and rate of PP were promoted by the PA-6 component because of its nucleating effect, whereas stepwise crystallization was detected for PA-6 in the PP/PA-6 blends when the TPE_g was added. On the basis of these observations, a schematic model was proposed for these blends. © 2003 Wiley Periodicals, Inc. J Appl Polym Sci 91: 1806–1815, 2004

Key words: elastomers; polyamides; poly(propylene) (PP); blends

INTRODUCTION

It has been estimated that the usage of polymers, regarded as the fastest growing structural materials, will grow 10% annually in the future. Polymer blends and alloys, which have been estimated to have increased 9% annually during past years, are widely used because of their excellent mechanical, thermal, and chemical properties (or some other specific properties) and their friendly processing conditions. The properties of polymer blends are intimately related to the characteristics of the components, the compositions, and the morphologies. During the past decades, much work has been dedicated to reaching a desired morphology through optimization of the processing conditions, including the process temperature, residence time, shear rate, and elongation draw, or through the reduction of the interfacial energy with an interfacial agent.[1]

Polypropylene (PP) and polyamide (PA) blends have been widely studied because these blends can combine the good thermal and mechanical properties of PA and the excellent processability and resistance to moisture of PP. However, the differences in the polarity and crystal structure of PP and PA can result in bad compatibilization between the two components. To obtain more homogeneous PP/PA blends through the addition of either interfacial active block copolymers or functionalized components, which react with the blends during the process, has become the dream of many researchers. For instance, the formation of bonds between maleic anhydride-*g*-polypropylene (PP_g) and polyamide 6 (PA-6) was investigated by Bidaux et al.[2] Reinforced PP was prepared by the blending of 70 vol % PP and 30 vol % PA-6 in the presence of compatibilizers, such as PP_g and maleic anhydride grafted rubbers.[3] The rheological properties, crystallization, and morphology of isotactic PP/PA-6 compatibilized with PP_g were investigated.[4] Static mechanical and falling weight impact tests were performed on PP/PA-6 blends compatibilized with PP_g.[5] Heino et al.[6] studied the fracture toughness of PA-6/PP blends to which SEBS-*g*-MA had been added. The compatibility of PP/PA-6 and PP/polyamide 6,6 with styrene–ethylene–butylene–styrene (SEBS) as an interfacial agent was found to be poor, but it became very good when SEBS-*g*-MA was used.[7] A copolymer consisting of PP grafted with phenol formaldehyde was found to be suitable for PP/PA-6 blends.[8]

In our laboratory, comprehensive studies have been performed on polymer composites and blend materials in the past decades. Rigid fillers in the polymers have been found to produce high-modulus, high-strength polymer composites, but they cannot improve the toughness. However, elastomers added to

Correspondence to: G. Yang (ygs@geniuscn.com).
Contract grant sponsor: National Natural Science Foundation of China.

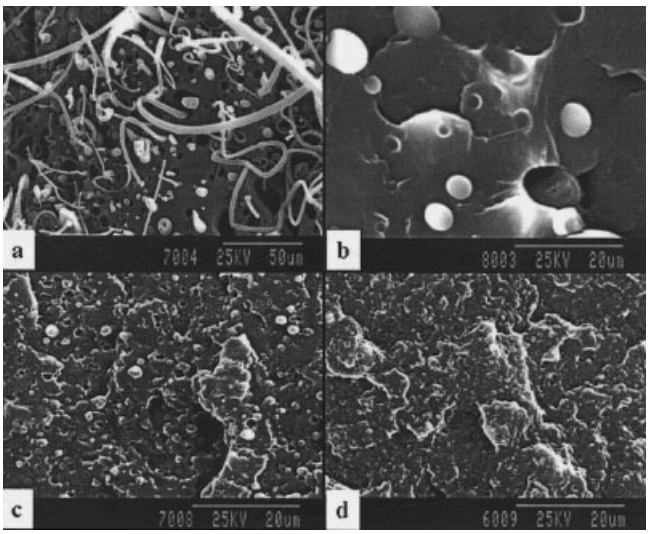

Figure 1 SEM micrographs of (a,b) PP/PA-6 (70/30 w/w), (c) PP/TPE_g (75/25 w/w), and (d) PP/PA-6/TPE_g (55/30/15 w/w/w).

the polymers easily increase the toughness but greatly reduce the stiffness. For the production of materials with high toughness, strength, and modulus, a thermoplastic matrix/elastomer/rigid filler system has been designed. Two kinds of phase structures can be expected in these blends: (1) the filler and elastomer separately dispersed in the matrix and (2) the filler as a core and the elastomer as a shell. Matonis[11] pointed out that it was doubtful that a mixture of separately dispersed phases of a filler and a elastomer, exhibiting two different and distinct responses to an applied load, could result in a composite with desirable properties. The encapsulation method was suggested.[9] Three factors can greatly affect the performance of this filler core/elastomer shell/thermoplastic matrix polymer composite: (1) the thickness of the elastomer shell, (2) the properties of the material in this shell phase, and (3) the interfacial adhesion of the various phases.[10–15] A careful consideration of these factors can produce stiffer and tougher materials. We want to extend this idea to PP/PA-6 blends and make PP matrix/elastomer interlayer/PA-6 core blends. To reach this goal, the design of the elastomer interlayer is crucial. Our work on high-density polyethylene (HDPE)/ethylene–propylene–diene monomer (EPDM)/carbon black (CB) composites has shown that bad interfacial adhesion results in separated CB and EDPM phases in the HDPE matrix.[16] When an interfacial modifier is used, CB is capsulated in EDPM, and this forms a core–shell structure. The resulting blends have much better mechanical properties. Lu et al.[17] studied rubber-particle-toughened nylon 6 with styrene/maleic anhydride copolymers, styrene/acrylic acid copolymers, ethylene/acrylic acid as a compatibilizer.[17] The interfacial adhesion was found to be intimately related to the final properties. A good compatibilizer should have both good reactivity with nylon 6 and miscibility with the core. The lack of either characteristic in a potential compatibilizer will presumably lead to a failure to provide an adequate dispersion of the core phase or interfacial adhesion. Our work has further shown that a soft interlayer of a certain thickness and good interfacial adhesion will improve the adhesion and mechanical properties.

We have developed a maleic anhydride grafted thermoplastic elastomer (TPE_g) consisting of maleic anhydride grafted poly(octene ethylene) (POE) rubber and a semicrystalline polyolefin. The incorporation of a semicrystalline polyolefin with POE not only improves the extruding processability and makes the resulting extrudate (TPE_g) easily pelletized but also lowers the cost. TPE_g has been shown to be an excellent elastomer for toughening PA-6. The POE part in TPE_g is an excellent interlayer for the PP/POE/talc ternary composite.[18–21] In this work, we used TPE_g as the interfacial agent for PP/PA-6 blends and studied its effect on the compatibility, morphology, and mechanical performance of the blends. The idea of using a soft elastomer as an interlayer for two rigid plastics was demonstrated.

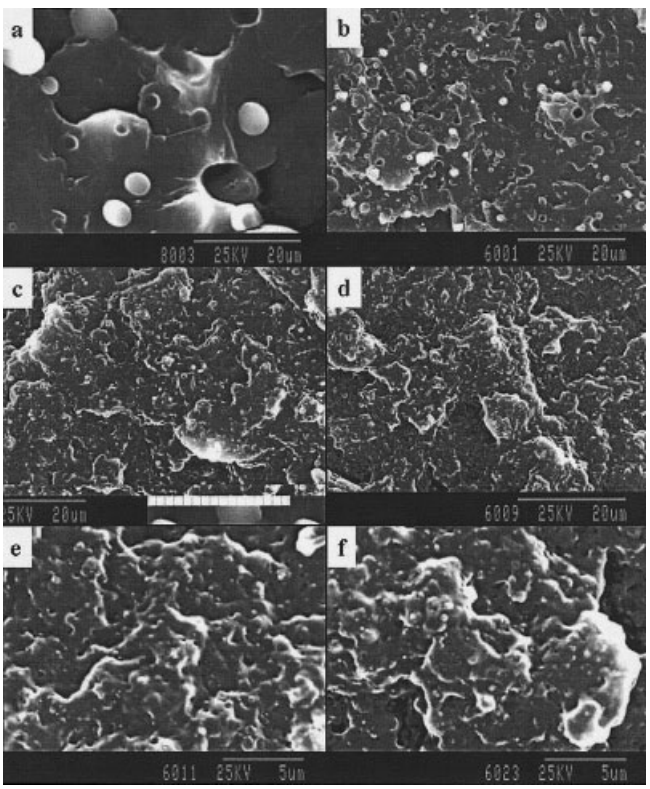

Figure 2 SEM micrographs of (a) PP/PA-6 (70/30 w/w), (b) PP/PA-6/TPE_g (64/30/6 w/w/w), (c) PP/PA-6/TPE_g (58/30/12 w/w/w), (d) PP/PA-6/TPE_g (52/30/18 w/w/w), (e) PP/PA-6/TPE_g (46/30/24 w/w/w), and (f) PP/PA-6/TPE_g (40/30/30 w/w/w).

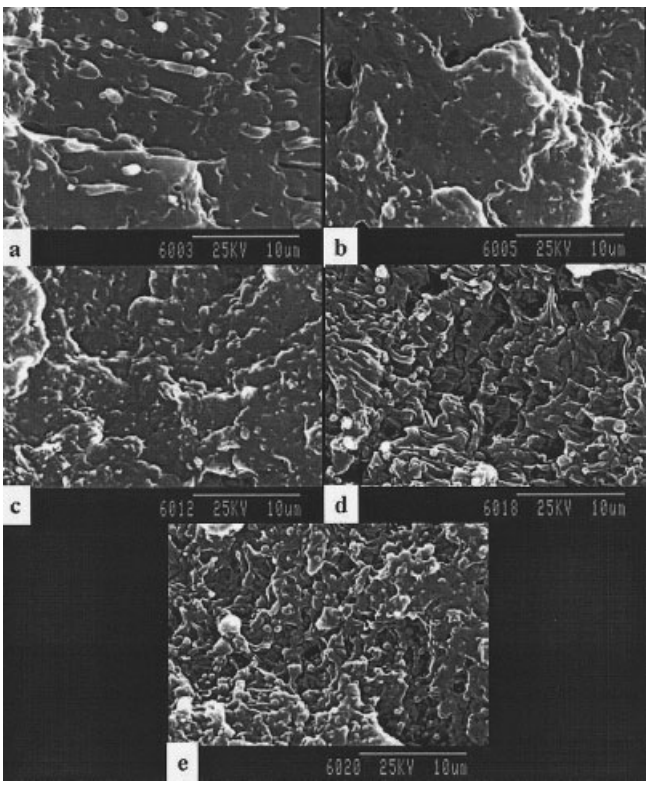

Figure 3 SEM micrographs of (a) PP/PA-6/TPE_g (64/30/6 w/w/w), (b) PP/PA-6/TPE_g (58/30/12 w/w/w), (c) PP/PA-6/TPE_g (52/30/18 w/w/w), (d) PP/PA-6/TPE_g (46/30/24 w/w/w), and (e) PP/PA-6/TPE_g (46/30/24 w/w/w).

EXPERIMENTAL

Materials

For TPE_g, the grafted maleic anhydride content, with respect to the blend, was about 1 wt %. POE (Engage 8445) was supplied by Dow Chemical China, Ltd. (Beijing, China). Its octane content and melt-flow rate were 9.5% and 3.5 g/10 min, respectively. TPE denotes a POE rubber/semicrystalline polyolefin (60/40) blend. PP (PP2401; Yanshan Petroleum & Chemical Co.) and PA-6 (Shanghai No. 18 Nylon Factory, Shanghai, China) were used as received.

Blend preparation

The blends were prepared by melt extrusion with a ϕ 30 twin-screw extruder (SHJ-30, Nanjing Plastic Machinery Co., Ltd., Nanjing, China) at 250 rpm. The barrel temperature was 220°C. The blends were pelletized, dried, and injection-molded into standard tensile, flexural, and Izod impact test specimens with an injection-molding machine (SZ-160/80 NB, Ningbo Plastics Machinery Co., Ltd., Ningbo, Zhejiang Province, China) at 220°C

Mechanical testing

The tensile and flexural tests were carried out on a universal tensile tester (Instron 1122, Instron, Ltd., England) according to National Standard Test Methods GB 1040-79 and GB 1042-79, respectively. The two test methods were very similar in their sample dimensions and test conditions to ASTM D 638 and ASTM D 790, respectively. The notched Izod impact strength was measured with an impact test machine (Custom Scientific Instruments CSI-127C, Atlas Electric Devices Co.) according to GB 1843-80, which is similar to ASTM D 256.

Thermal analysis

Nonisothermal scans were carried out on a PerkinElmer DSC-7 differential scanning calorimeter at a heating or cooling rate of 20°C/min from 25 to 260°C under an N_2 purge. The nylon samples were dried *in vacuo* at 80°C for 12 h before the analysis.

Morphological observations

The impact-fractured surfaces of the blends samples at room temperature were observed with a Hitachi S-530 scanning electron microscope. The surfaces were coated with gold.

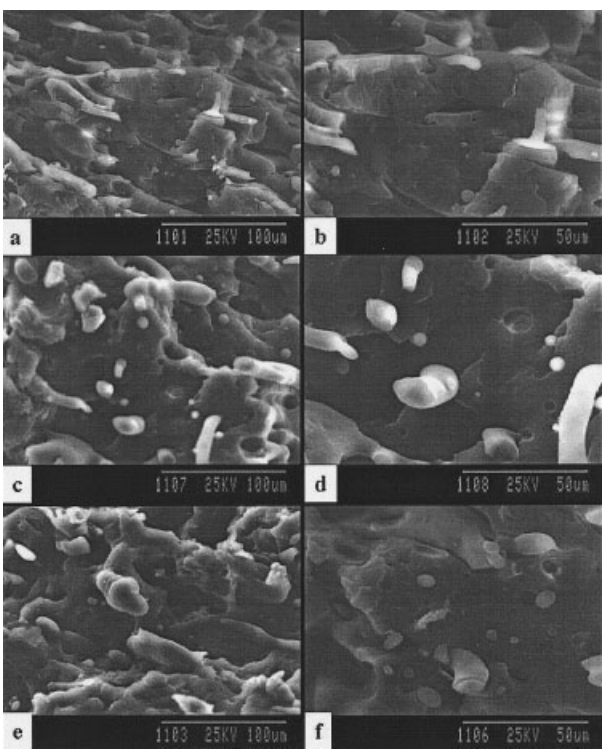

Figure 4 SEM micrographs of (a,b) PP/PA-6/TPE (64/30/6 w/w/w), (c,d) PP/PA-6/TPE (52/30/18 w/w/w), and (e,f) PP/PA-6/TPE (46/30/24 w/w/w).

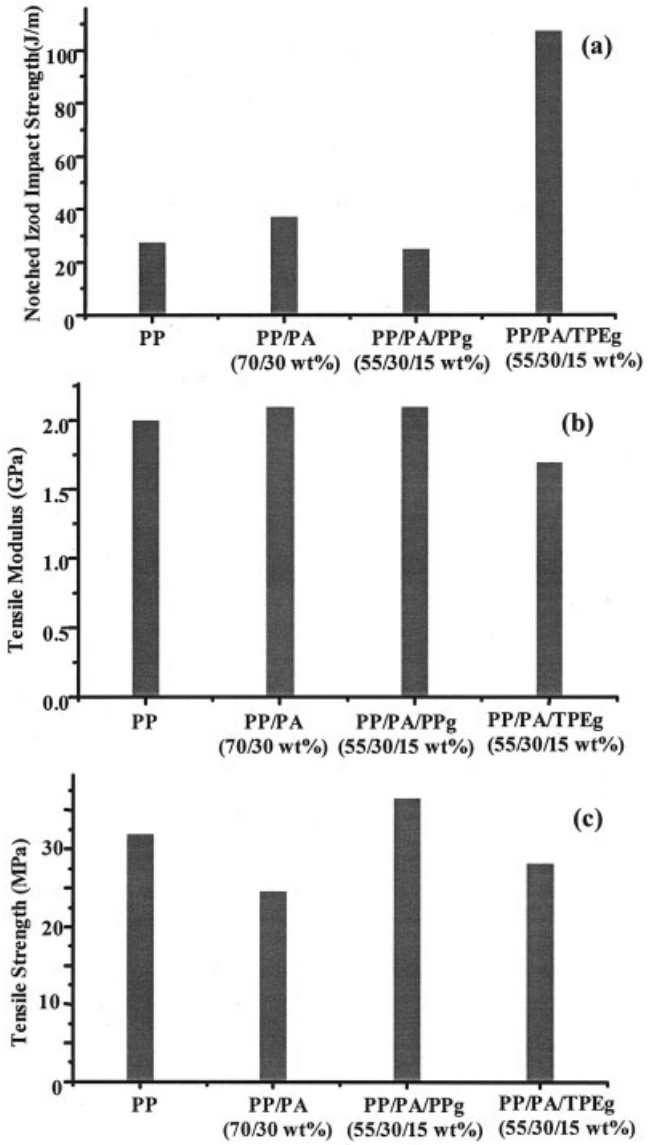

Figure 5 Mechanical properties of PP and PP/PA-6 blends.

Dynamic mechanical analysis

A dynamic mechanical analyzer (DMA-7, PerkinElmer) was used to measure the dynamic mechanical properties of the blends. The specimens were 3 mm × 10 mm × 1.5 mm. Before the measurements were taken, the specimens were dried in a vacuum oven for 12 h at 80°C. Temperatures from −170 to 160°C were used in a three-point bending mode at a vibration frequency of 1 Hz and at a heating rate of 5°C/min in a nitrogen atmosphere.

RESULTS AND DISCUSSION

Morphology

To test the efficiency of TPE_g as a compatibilizer for PP/PA-6 blends, we investigated the microstructures of the blends with scanning electron microscopy (SEM). The microstructures of PP/PA-6, PP/TPE_g, and PP/PA-6/TPE_g are illustrated in Figure 1. Each micrograph was taken at the surface with a thin coating of gold after the impact test. PP and PA-6 had poor compatibilization because of the differences in the polarity and crystal structure. In the PP/PA-6 blends without TPE_g, PA-6 domains with diameters of 7–10 μm were dispersed in the continuous PP matrix. The long PA-6 fibers shown in the micrographs were formed because of the elongation during the impact test. Partial PA-6 phases were completely dislodged, leaving dark voids in the matrix [Fig. 1(a,b)]. Big cracks can be clearly seen between the PP and PA-6 phases. Although they had similar backbone structures, TPE_g had only moderate compatibilization with PP [Fig. 1(c)]. TPE_g particles were dispersed in the PP matrix with diameters of 3–4 μm (3.5 μm on average). Many TPE_g particles were exposed, and this indicated only moderate adhesion between PP and TPE_g. Our early work showed that POE had good miscibility with PP. Therefore, the diminished miscibility between PP and TPE_g must have resulted from the functionalization of POE by the succinic anhydride groups, which raised the polarity, charge, and hydrophilicity.

With the addition of 15 wt % TPE_g to PP/PA-6, the morphologies changed obviously. No PA-6 fibers existed again. The PA-6 particle size was reduced to 1 μm, and the particle size range was very small. The particles were dispersed quite uniformly over the matrix [Fig. 1(d)]. TPE_g greatly improved the dispersion of the PA-6 phase. During the blending process, the succinic anhydride groups of TPE_g reacted with the amino groups of PA-6, and this resulted in grafted copolymers, which had a strong tendency to be anchored at the PP/PA-6 interface. Most of the succinic groups of TPE_g were incorporated into PA-6, and the miscibility between PP and TPE_g was improved because of the disappearance of the polarity groups in TPE_g.

The microstructures of PP/PA-6 blends with various amounts of TPE_g are shown in Figure 2. Increasing the amount of TPE_g changed the following features: (1) PA-6 fibers found in uncompatibilized PP/PA-6 [Fig. 1(a)] disappeared when TPE_g was used [Fig. 2(b)], (2) the PA-6 domain size was reduced when the TPE_g content was increased, (3) the PA-6 domains size was smaller when more TPE_g was used, and (4) PA-6 was dispersed more and more uniformly through the addition of more TPE_g. These features well reflected how TPE_g could improve the dispersion of PA-6 in the PP matrix.

Figure 3 provides a close look at the microstructures with higher resolution micrographs. For blends with less than 24 wt % TPE_g, the impact-fractured surfaces were very smooth, this being characteristic of brittle polymers. The impact energy was mainly dissipated

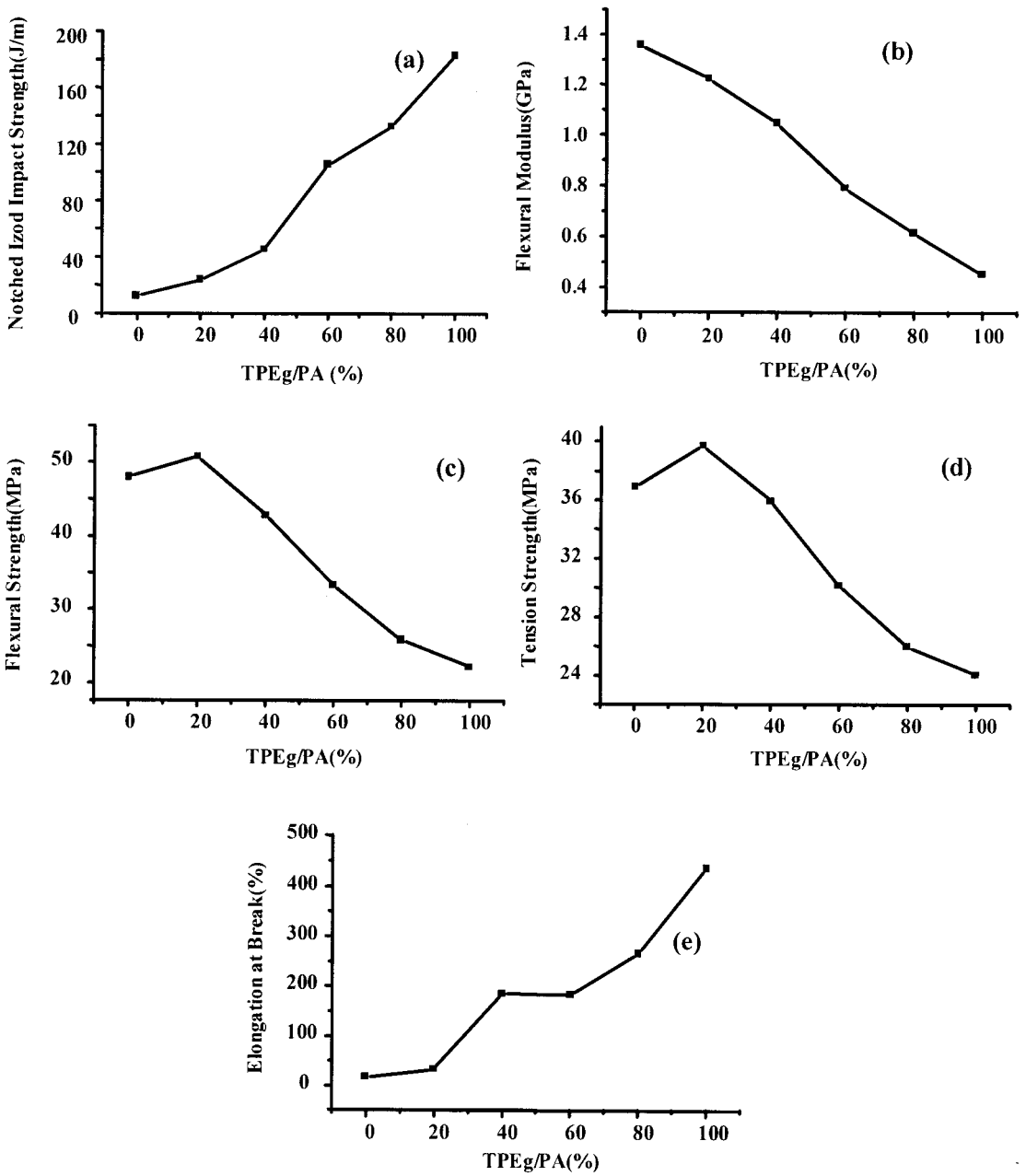

Figure 6 Effects of the TPE_g/PA-6 ratio on the mechanical properties of PP/PA-6/TPE_g blends (all blends had 30 wt % PA-6).

through matrix crazing. For blends with 24 and 36 wt % TPE_g, profuse cavitation and matrix shear yielding can be observed.

For PP/PA-6/TPE blends, the phase structures were quite different. Three phases, including continuous, fibrous, and spherical phases, were clearly found in the blends (Fig. 4). We attributed the continuous matrix to PP and the fibers to PA-6 based on PP and PA-6 compositions in the blend. Uncompatibilized PP/PA-6, having PA-6 fibers, provided further proof of this. The spherical particles were mainly attributed to TPE because the number and total volume of this phase rose as the TPE content increased. Partial particles may have been PA-6; the diameters of the PA-6 fibers and the dispersed particles did not change much as more TPE was used. The interface between PP and PA-6 was kept clear. Although TPE had good miscibility with PP, TPE could not react with PA-6 because of the lack of succinic anhydride groups. As a result, TPE could not form a core–shell structure with PA-6 and improve the dispersion of PA-6 in the PP matrix. A typical isolated three-phase structure was formed.

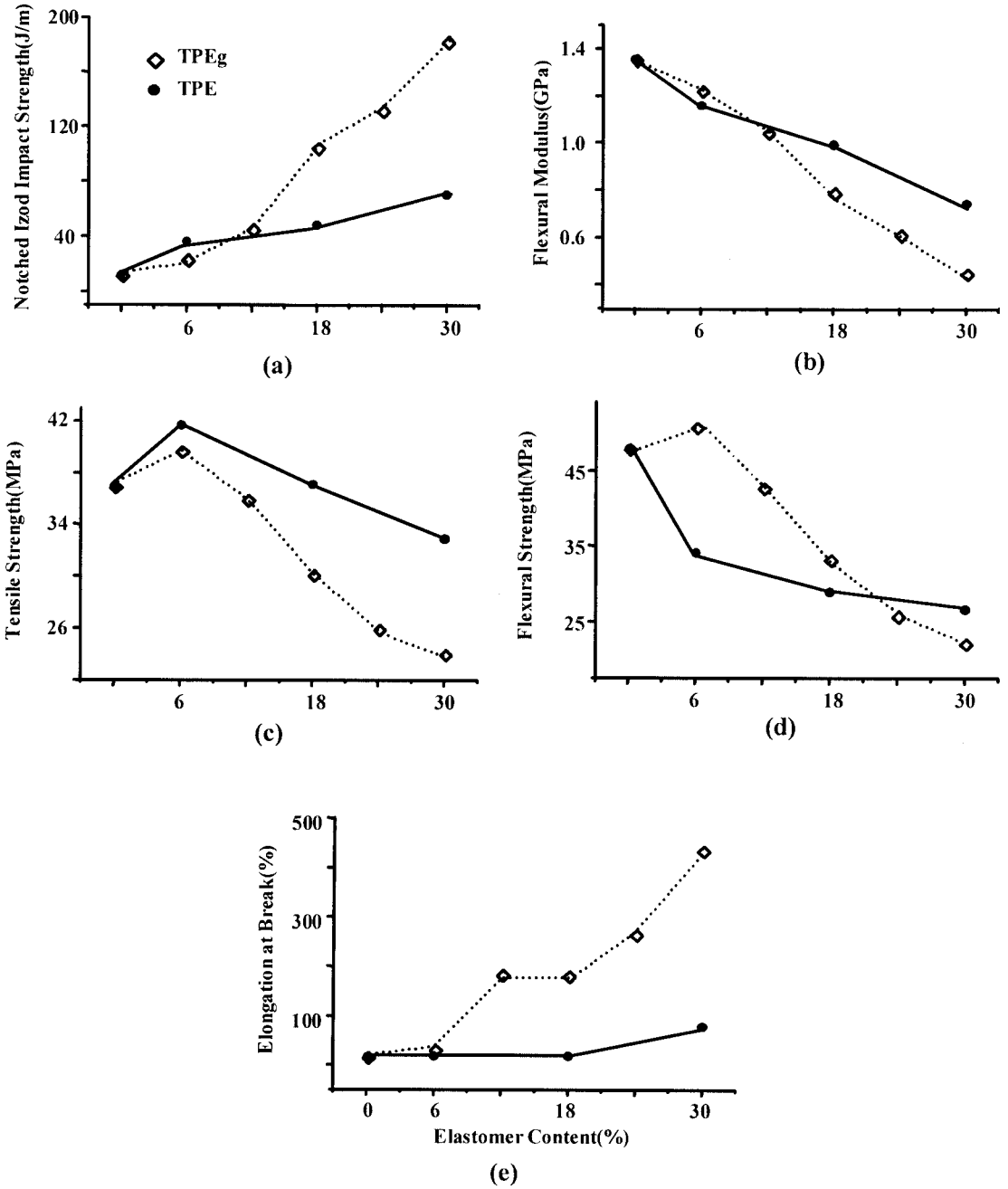

Figure 7 Effect of the TPE_g (TPE) content on the mechanical properties of PP/PA-6/TPE_g (TPE) blends (all blends had 30 wt % PA-6).

Mechanical properties

As an interfacial modifier, TPE_g could affect the final properties of the blends in three ways. First, TPE_g improved the dispersion of the PA-6 domains, reduced the PA-6 domain size, and reduced the dispersed particle–particle distance. These could influence the toughness of the blends. As shown in many rubber-toughened pseudoductile polymers, there is a critical particle–particle distance. Blends with dispersed particle–particle distances less than this critical distance will transform from brittle polymers into ductile polymers. In our PP/PA-6/TPE_g blends, PA-6 surrounded with a TPE_g elastomer layer could act as a particle, toughening the PP matrix. Therefore, the improved dispersion could significantly change the toughness of PP. Second, TPE_g increased the interfacial adhesion of PP and PA-6. The succinic anhydride groups in TPE_g reacted with the amino groups of PA-6. POE in TPE_g was dissolved in the PP matrix. Third, the thick soft TPE_g layer contributed to the final

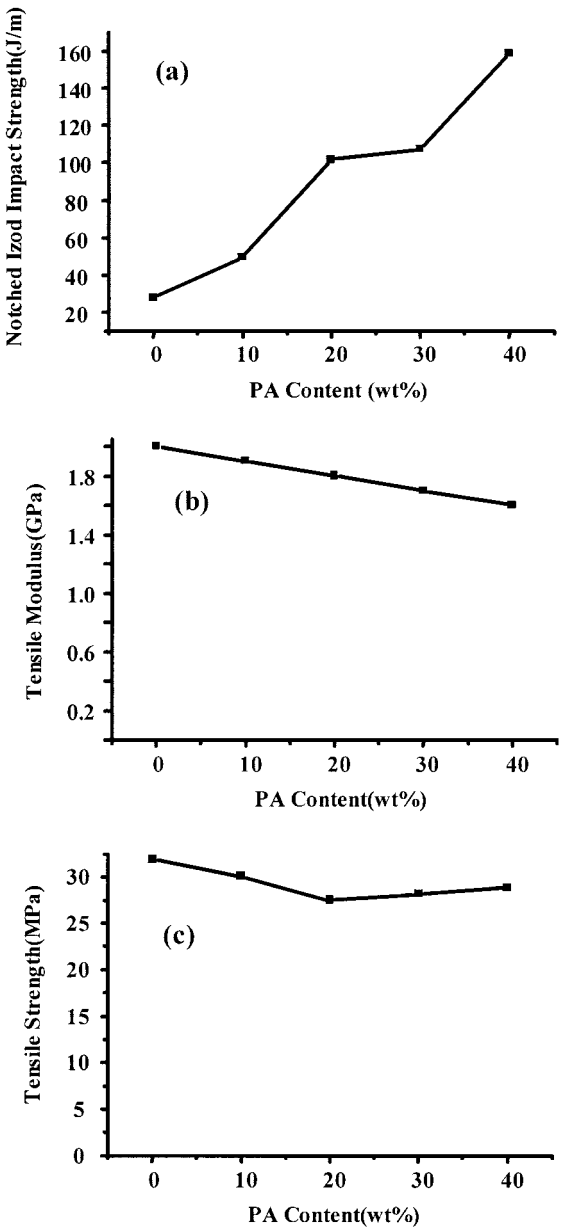

Figure 8 Effects of the PA-6 content on the mechanical properties of PP/PA-6/TPE_g blends (the TPE_g/PA-6 ratio was fixed at 1/2 for all the blends).

mechanical properties, increasing the toughness and lowering the modulus. In the following paragraphs, we examine the effectiveness of TPE_g as an interfacial modifier and then characterize the effects of the interlayer structure on the mechanical properties.

To test the efficiency of TPE_g as an interfacial agent for the PP/PA-6 blends, we characterized the mechanical properties of the PP/PA-6 blends. Figure 5 illustrates the notched Izod impact strength, tensile modulus, and tensile strength of different samples. PP/PA-6 consisted of 70 wt % PP and 30 wt % PA-6. The TPE_g-compatibilized PP/PA-6 was 55 wt % PP, 30 wt % PA-6, and 15 wt % TPE_g. The properties of PP_g-compatibilized PP/PA-6 are listed as well.

PP and PA-6 were brittle polymers with notched Izod impact strengths of 28 and 19 J/m, respectively. Simply blending PP and PA-6 did not improve the mechanical properties. With respect to pure PP, the notched Izod impact strength and tensile modulus only slightly increased, whereas the tensile strength was actually reduced. The difference in the polarity and crystal structure of PP and PA-6 led to a high interfacial energy and bad adhesion between the two components. The mechanical properties confirmed the poor compatibilization of PP and PA-6, as shown in the SEM micrographs.

Adding 15 wt % TPE_g into the PP/PA-6 blends increased the notched Izod impact strength to 110 J/m, which was nearly 3 times that of unmodified PP/PA-6. The tensile strength was also improved from 25 to 28 MPa. However, the blend with a 110 J/m notched impact strength was still brittle, and this agreed well with the smooth impact-fractured surface shown in Figure 1(d).

PP_g was used as a stiff interfacial agent in this study. As expected, the tensile modulus and strength improved, but the toughness deteriorated.

In the PP/PA-6/TPE_g blends, TPE_g was expected to surround the dispersed PA-6 domains and be located at the interface of PP and PA-6. Therefore, the TPE_g/PA-6 weight ratio would determine the thickness and structure of the interlayer. Large amounts of TPE_g could produce more succinic anhydride to react with

TABLE I
Nonisothermal Crystallization of PP and PA-6 in the PP/PA-6/TPE_g Blends

		PP			PA-6		
Sample	Composition (wt %)	T_c (°C)	ΔH_c (J/g)	Crystallinity (%)	T_c (°C)	ΔH_c (J/g)	Crystallinity (%)
PP	100	116.9	−98.7	47.19			
PP/PA-6	70/30	120.2	−105.5	50.44	191.2	−55.67	34.80
PP/TPE_g	75/25	116.7	−106.0	50.71			
PP/PA-6/TPE_g	64/30/6	121.7	−103.5	49.27	187.7	−67.30	42.08
PP/PA-6/TPE_g	52/30/18	118.5	−116.9	55.90	185.8	−6.28	3.93
PP/PA-6/TPE_g	40/30/30	117.8	−152.0	72.67	186.7	−1.34	0.84

TABLE II
Nonisothermal Crystallization of PP and PA-6 in the PP/PA-6/TPE Blends

		PP			PA-6		
Sample	Composition (wt %)	T_c (°C)	ΔH_c (J/g)	Crystallinity (%)	T_c (°C)	ΔH_c (J/g)	Crystallinity (%)
PP/PA-6	70/30	120.2	−105.5	50.44	191.2	−55.67	34.80
PP/PA-6/TPE	64/30/6	121.7	−111.6	53.34	191.1	−56.20	35.14
PP/PA-6/TPE	52/30/18	121.7	−131.4	62.85	191.2	−56.07	35.05
PP/PA-6/TPE	40/30/30	121.6	−132.5	63.33	191.0	−51.37	32.12

PA-6. It had more POE dissolved in the PP matrix as well. As a result, large amounts of TPE_g increased the interfacial interaction. Large amounts of TPE_g formed a thick soft interlayer as well. The layer improved the toughness and reduced the modulus. Figure 6 shows the influence of the TPE_g/PA ratio on the final mechanical properties. All the blends had 30 wt % PA-6. The TPE_g/PA-6 ratio increased the notched Izod impact strength linearly. However, the TPE_g elastomer made a negative contribution to the tensile and flexural properties.

Figure 7 further shows the effects of the TPE_g percentages in the blends on their final performance. PA-6 was fixed at 30 wt % in all the blend samples. The ungrafted TPE is presented as well. TPE_g improved the notched Izod impact strength linearly, whereas TPE only slightly changed the properties.

The PA-6 content in the blends was another important factor affecting their properties and price, and it is studied in Figure 8. The notched Izod impact strength, tensile modulus, and strength were plotted versus the PA contents in the PP/PA-6/TPE_g blends. TPE_g/PA-6 was fixed to be 1/2, at which ratio there was enough TPE_g to compatibilize PP/PA-6. The notched impact strength grew linearly with respect to the PA-6 content. The tensile strength and modulus only slightly changed.

These results show that TPE_g acted as a high-efficiency interfacial agent for the PP/PA-6 blends. The TPE_g/PA-6 ratios and TPE_g and PA-6 percentages in the blends were intimately related to the final properties. The careful design of PP, PA-6, and TPE_g produced blends with expected properties, whereas ungrafted TPE polymer altered the blends slightly.

Thermal properties

The nonisothermal crystallization and melting of PP/PA-6/TPE_g blends were studied. The heat, temperature of crystallization, and crystallinity of PP and PA-6 are listed in Table I. In a binary polymer blend system, the crystallization temperature (T_c) of the major component is often increased. The possible reasons accounting for this behavior are (1) the migration of nuclei across the interface from the minor component to the major component, (2) the nucleating-agent-like behavior of the existing crystal of the minor component, (3) the alternation of the chain mobility at the interface, (4) the loss of the molecular weight during the mixing process. Pure PP crystallized at 116.9°C. T_c of PP in the PP/PA-6 blend was boosted to 120°C, whereas T_c of PP in the PP/TPE_g blends was kept at 116.7°C. These results indicated that PA-6 could promote the nucleation of the PP matrix, whereas TPE_g could not. For the PP/PA-6/TPE_g blends, when 6 wt % TPE_g was used, T_c of PP was 121.7°C, which was close to that of PP/PA-6. PA-6 had a strong nucleating effect on PP. When 18 wt % TPE_g was added, T_c of PP was 118.5°C; when 30 wt % TPE_g was added, T_c of PP was 117.8°C, which was very close to that of pure PP. These results showed that a thick TPE_g layer surrounded the PA-6 phase and reduced the nucleating effect of PA-6 to PP when more than 18 wt % TPE_g was added. The thick TPE_g layer isolated PA-6 from the PP matrix, prevented the migration of nuclei across the interface, or weakened the nucleating effect of PA-6 to PP.

It is well known that fractionated crystallization often occurs in PP/PA blends.[22–26] For semicrystalline polymers, primary nucleation is usually the rate-determining step. The crystal rapidly grows over the materials once it is nucleated. In blends with a well-dispersed minor component, if the number of dispersed particles is greater than the number of general active nucleating heterogeneities (A_1) within the blends, the nucleation in the particles without A_1 can only rely on another type of heterogeneity (A_2), for which a lower T_c is needed, or the crystallization in these particles without A_1 is retarded until a homoge-

TABLE III
Dynamic Mechanical Behavior of PP and PA-6 in the PP/PA-6/TPE_g Blends

Sample	Composition (wt %)	T_g of PP (°C)	T_g of PA-6 (°C)	ΔT_g (°C)
PP/PA-6	70/30	14.2	80.8	66.6
PP/PA-6/TPE_g	64/30/6	25.2	82.2	57.0
PP/PA-6/TPE_g	52/30/18	24.5	89.9	65.4
PP/PA-6/TPE_g	40/30/30	18.4	98.2	79.8

TABLE IV
Dynamic Mechanical Behavior of PP and PA-6 in the PP/PA-6/TPE Blends

Sample	Composition (wt %)	T_g of PP (°C)	T_g of PA-6 (°C)	ΔT_g (°C)
PP/PA-6	70/30	14.2	80.8	66.6
PP/PA-6/TPE	64/30/6	13.2	73.3	60.2
PP/PA-6/TPE	52/30/18	9.8	69.3	59.5
PP/PA-6/TPE	40/30/30	9.1	75.8	66.8

neous nucleation begins, for which a further lower T_c is demanded. The crystallization of the minor component may, therefore, take place during several steps. Sometimes, the crystallization of the minor component occurs coincidently with the major component, and the crystallization peaks of PP and PA-6 overlap. In our PP/PA-6/TPE_g blends, using TPE_g led to a very fine dispersion of PA-6. The crystallization of the PA-6 phase was divided into several steps. The first crystallization occurred about 5°C lower than the usual T_c of pure PA-6. The decrease in T_c may have been due to the diluting effect of PP and TPE_g in the blends or due to the restricted PA-6 chain mobility from the grafting reaction with TPE_g. The second crystallization took place coincidently with the crystallization of the matrix PP, in which PP and PA-6 could have a mutual nucleating effect. When more than 18 wt % TPE_g was added into the blends, the first crystallization was almost completely suppressed. Meanwhile, the crystallinity of PP increased dramatically, and this was partially due to the second step of crystallization of PA-6. These differential scanning calorimetry results agreed well with the microstructures of the blends revealed by SEM and could be applied to estimate the compatibilities of the blends. However, the melting behaviors of the different blends were almost the same, and so it was concluded that the total crystallinity of PA-6 was nearly not changed for blends with different TPE_g contents and that PP and PA-6 crystallized separately.

The nonisothermal crystallization and melting data of PP/PA-6/TPE blends are listed in Table II. PA-6 improved the nucleation of PP. T_c, the crystallinity, and the crystallization heat increased as the PA content increases. TPE had no effect on the crystallization of PP. PP and TPE did not influence the crystallization behavior of PA-6. These findings agreed well with the isolated three-phase structure of the blends.

Dynamic mechanical properties

The dynamic thermal mechanical properties are listed in Tables III and IV. Adding TPE_g to the blend system raised the glass-transition temperatures (T_g's) of PP and PA-6. The physical or chemical interactions between PP, PA-6, and TPE_g at the interface reduced the mobility of PP and PA-6 and led to increases in T_g. Obviously, the interaction between TPE_g and PA-6 was much stronger than that between PP and PA-6. The PA-6 chains reacted with TPE_g, and this led to TPE_g-grafted PA-6. The mobility of the PA-6 segments was significantly restricted. As a result, T_g of PA-6 was greatly improved. TPE had no strong interactions either with PP or with PA-6. TPE in the blend system increased the free volume of both PP and PA-6, producing a drop in T_g. Figure 9 shows the process pressure of the PP/PA-6/TPE_g and PP/PA-6/TPE blends. When TPE_g was added, the grafting reactions between TPE_g and PA-6 and the entanglements between TPE_g and PP led to a higher viscosity, thus increasing the process pressure.

Schematic model

On the basis of the aforementioned mechanical and thermal behaviors and the microstructures revealed by SEM, a schematic model for the PP/PA-6/TPE_g and PP/PA-6/TPE blends is presented in Scheme 1. For PP/PA-6/TPE_g, TPE_g had strong interactions with both PP and PA-6. TPE_g was located at the interface between PP and PA-6 as the interlayer. For samples with 30 wt % TPE_g or more, most PA-6 reacted with TPE_g to form a dispersed phase. For the PP/PA-6/TPE blend, TPE had no strong interactions with PP and PA-6. TPE formed an isolated phase in the PP matrix. These results agreed well with our initial intention to use the TPE_g elastomer as an interlayer between PP and PA-6.

CONCLUSIONS

TPE_g, an elastomer prepared and used in a former study, could greatly toughen PA-6. In this study, we

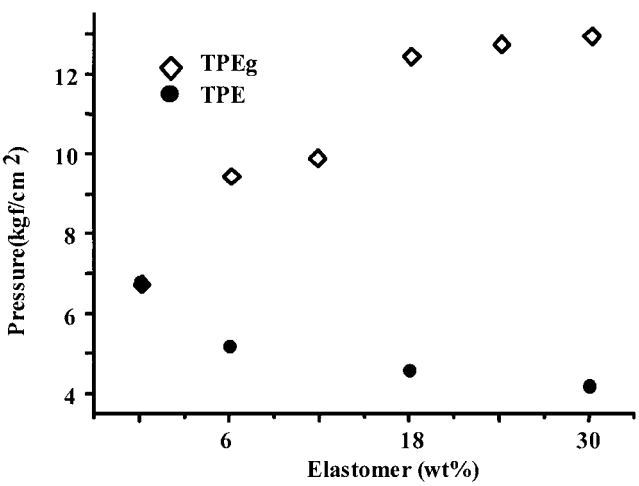

Figure 9 Processing pressure of PP/PA-6/TPE_g blends with various elastomer contents (all blends had 30 wt % PA-6).

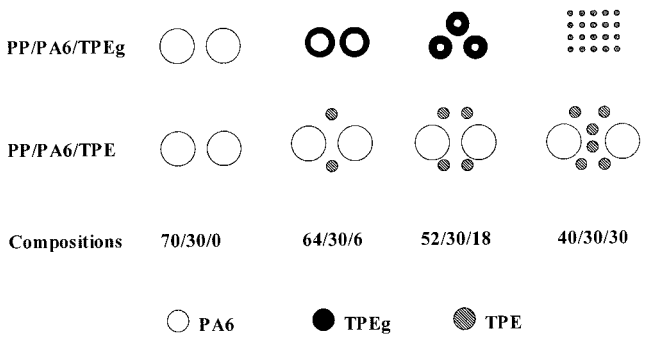

Scheme 1 Schematic microstructures for PP/PA-6/TPE_g and PP/PA-6/TPE blends.

used TPE_g to improve the compatibility of PP and PA-6. TPE_g could greatly improve the toughness but only slightly reduced the tensile strength and modulus of PP/PA-6 blends when 15 wt % TPE_g was added. The TPE_g/PA-6 ratio influenced the interfacial structure and adhesion. SEM micrographs showed that TPE_g was located at the interface of PP and PA-6 in the PP/PA-6/TPE_g blends, whereas for the PP/PA-6/TPE blends, a three-phase structure was formed. T_c and the rate of PP in the PP/PA-6/TPE_g blends increased with the PA-6 component because of the nucleating effect. For the minor phase PA-6, a two-step crystallization was detected. The first crystallization occurred at a temperature lower than T_c of pure PA-6 because of the dilute effect of PP and TPE_g or the reduced mobility of PA-6 chains resulting from the grafting reaction. The second crystallization happened coincidently with the crystallization of PP. The strong interactions between PP, PA-6, and TPE_g at the interface reduced T_g of PP and PA-6. These results show that using soft elastomers as interfacial layers between rigid components is an effective way of preparing high-quality materials.

References

1. Utracki, L. A. Polym Eng Sci 1995, 35, 2.
2. Bidaux, J. E.; Smith, G. D.; Bernet, N.; Manson, J. A. D.; Hilborn, J. Polymer 1996, 37, 1129.
3. Rosch, J.; Mulhaupt, R. Adv Chem Ser 1996, 252, 291.
4. Marco, C.; Ellis, G.; Gomez, M. A.; Fatou, J. G.; Arribas, M.; Campoy, I.; Fontecha, A. J Appl Polym Sci 1997, 65, 2665.
5. Tjong, S. C. J Mater Sci 1997, 32, 4613.
6. Heino, M.; Hietaoja, P.; Seppala, J.; Harmia, T.; Friedrich, K. J Appl Polym Sci 1997, 66, 2209.
7. Ohlsson, B.; Hassander, H.; Tornell, B. Polymer 1998, 39, 6705.
8. Borve, K. L.; Kotlar, H. K.; Gustafson, C. G. J Appl Polym Sci 2000, 75, 355.
9. Kolarik, J.; Jancar, J. Polymer 1992, 33, 4961.
10. Broutman, C. J.; Agarwal, B. D. Polym Eng Sci 1974, 14, 581.
11. Matonis, V. A.; Small, N. C. Polym Eng Sci 1969, 9, 90.
12. Pfeiffer, D. G.; Nielsen, L. E. J Appl Polym Sci 1979, 23, 2253.
13. Pfeiffer, D. G. J Appl Polym Sci 1979, 24, 1451.
14. Jean-Baptiste, D. Pure Appl Chem 1981, 53, 2223.
15. Arridge, R. G. C. Polym Eng Sci 1975, 15, 757.
16. Ou, Y. C.; Zhu, J.; Feng, Y. P. J Appl Polym Sci 1996, 59, 287.
17. Lu, M.; Keskkula, H.; Paul, D. R. Polym Eng Sci 1994, 34, 33.
18. Yu, Z. Z.; Ou, Y. C.; Qi, Z. N.; Chen, G. H. J Polym Sci Part B: Polym Phys 1998, 36, 1987.
19. Yu, Z. Z.; Lei, M.; Ou, Y. C.; Hu, G. H. J Polym Sci Part B: Polym Phys 1999, 37, 2664.
20. Yu, Z. Z.; Lei, M.; Ou, Y. C.; Yang, G. S. Acta Polym Sinica 2000, 3, 275.
21. Lei, M.; Zhou, J. F.; Yu, Z. Z.; Ou, Y. C.; Yang, G. S. Acta Polym Sinica 2000, 5, 608.
22. Ikkala, O. T.; Holsti-Miettinen, R. M.; Seppala, J. J Appl Polym Sci 1993, 49, 1165.
23. Tang, T.; Huang, B. T. J Appl Polym Sci 1994, 53, 355.
24. Moon, H. S.; Ryoo, B. K.; Park, J. K. J Polym Sci Part B: Polym Phys 1994, 32, 1427.
25. Campoy, I.; Arribas, J. M.; Zaporta, M. A. M.; Marco, C.; Gomez, M. A. Eur Polym J 1995, 31, 475.
26. Pompe, G.; Potschke, P.; Pionteck, J. J Appl Polym Sci 2002, 86, 3445.